JACS
JOURNAL OF THE AMERICAN CHEMICAL SOCIETY

ARTICLE

pubs.acs.org/JACS

Ultrafast Geminate Recombination after Photodetachment of Aqueous Hydroxide

Hristo Iglev,* Martin K. Fischer, Alexander Gliserin, and Alfred Laubereau

Physik-Department E11, Technische Universität München, D-85748 Garching, Germany

Supporting Information

ABSTRACT: The photodetachment of aqueous hydroxide (OH^-_{aq} and OD^-_{aq}) is studied using femtosecond pump−probe and pump−repump−probe spectroscopy. The electron is detached after excitation of the hydroxide ion to a charge-transfer-to-solvent (CTTS) state at 202 nm. An early intermediate is observed that builds up within 160 fs and is assigned to nonequilibrated OH−electron pairs. The subsequent dynamics are governed by thermalization, partial recombination, and dissociation of the pairs, yielding the final hydrated electrons and hydroxyl radicals. An additional pulse at 810 nm is used for secondary excitation of the intermediate species so that more insight is gained into the recombination process(es). Using this technique we observe a novel geminate recombination channel of OH with adjacent hydrated electrons. This channel leads to ultrafast quenching (700 fs) of almost half the initial number of radicals. The fast mechanism displays an isotope effect of 1.4 (for OD^-_{aq} quantum yield 35%, time constant 1.0 ps). This process was not observed in similar experiments on aqueous bromide and seems to be related to the special properties of the hydroxide ion and its local H-bonding environment. Our findings underline the high reactivity of the prehydrated electron.

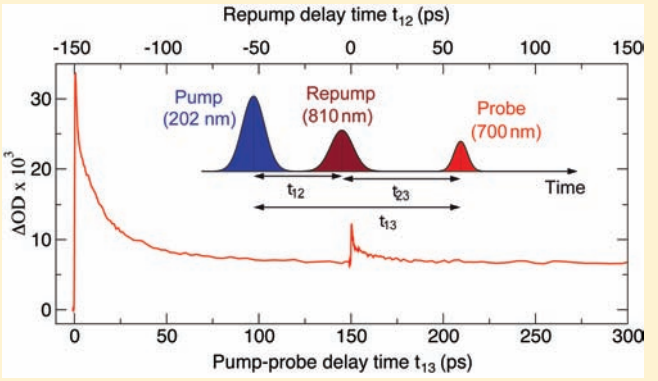

1. INTRODUCTION

The hydroxyl radical is the most powerful oxidizing radical in biological systems, and the mechanisms for its generation and scavenging attract particular scientific interest.[1−4] Recently, Wang et al.[5] reported dissociative electron transfer reactions of prehydrated electrons with DNA nucleotides in aqueous solution. The results demonstrate the crucial role of not fully hydrated electrons in many charge transfer reactions occurring in aqueous environments.[5−7] Different mechanisms for the photoionization of water at lower photon energies (<10 eV) have been proposed.[8,9] One of these mechanisms includes excited CTTS states of OH^-.[10] Therefore, the detailed understanding of the electron photodetachment of aqueous hydroxide is of special importance in life sciences.

The comprehension of the unusual structural and dynamical properties of the hydroxide ion on the microscopic level still attracts significant scientific interest.[11−16] The detachment threshold of the isolated OH^- is 1.83 eV,[17] while in aqueous solution the corresponding value increases to 9.2 eV.[18] The resulting high ionization threshold in solution is a prerequisite for the formation of a CTTS band centered at 6.6 eV.[19] An optical excitation in this band leads to an effective electron transfer from the hydroxide ion to the solvent.[20−22] The phenomenon is attributed to the large spatial extension of the CTTS wave function over the first solvent shell of the anion.[23] The photodetachment mechanism is believed[20] to be similar to those of halide ions in water.[24−31] The initially excited CTTS state is followed by a rapid (partial) separation of the residual electron with the transition to a weakly bound ($3-4k_BT$)[20,24,25] solvent-separated electron-donor pair.[32,33] The pair subsequently dissociates with a certain quantum yield, forming isolated (long-lived) species, a neutral donor, and a hydrated electron e^-_{hyd}.[22]

The solvent shell of OH^-_{aq} differs significantly from that of the aqueous halides.[34−36] The hydroxide is strongly bound to an average of 3−4 water molecules and experiences rapid proton transfer along the H-bonded network.[11−13] Thus, the OH^-_{aq} develops unique features among the hydrated anions. Recently, Petersen et al.[22] reported that 35% of the electrons excited into CTTS state relax to a "hot" OH^-_{aq} due to internal conversion. The observed time constant of 2 ps is significantly longer than the lifetime of the CTTS state reported for other systems.[25,37] A similar relaxation channel was not reported for any other hydrated anion, except fluoride,[37] and seems to be related to special properties of both anions and their local H-bonding networks.[15]

The initial relaxation process significantly reduces the quantum yield of the highly reactive OH radicals and quasi-free electrons. A deeper understanding of the mechanism and dynamics of this process is the main goal of the present work. For

Received: May 10, 2010
Published: December 28, 2010

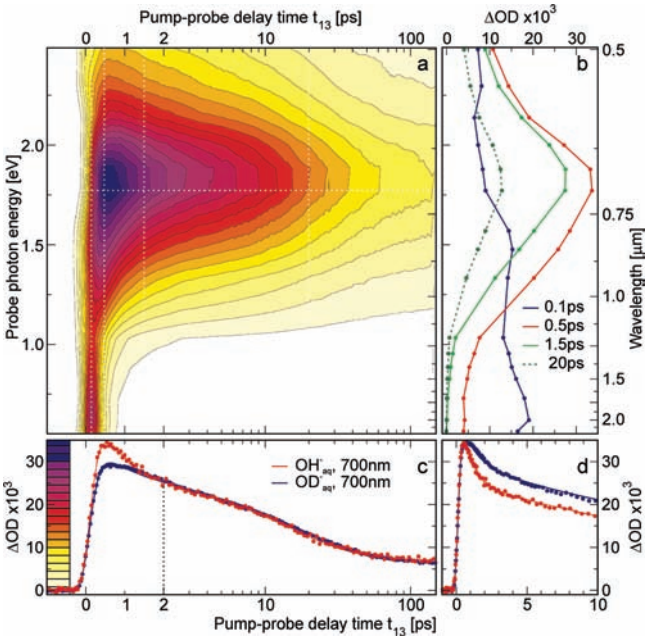

Figure 1. Pump−probe spectroscopy of aqueous hydroxide at room temperature. (a) Contour plot of the absorption changes measured in OH^-_{aq} as a function of pump−probe delay time and probe photon energy. The contour values are given in the color scale next to (c). Note the linear and logarithmic abscissa scales below and above 2 ps, respectively (same for (c)). (b) Transient spectra measured at fixed pump−probe delay times (see inset). (c and d) Signal transients at 700 nm for OH^- in H_2O (red) and OD^- in D_2O (blue). For a better view, the OD^-_{aq} data presented in (c) are scaled by a factor of 0.8. Experimental points, calculated solid lines.

this purpose the photodetachment of OH^-_{aq} and OD^-_{aq} is studied using pump−probe and pump−repump−probe (PREP) spectroscopy.[38] Excitation is performed by 1-photon absorption at 202 nm and the subsequent relaxation dynamics measured in the spectral range from 450 nm to 2.45 μm. The secondary excitation of the released electrons hinders their recombination with the donors. Thus, the long-time survival probability of hydrated electrons measured in the PREP experiment is higher than the one observed with a pump−probe technique. The PREP data give evidence of the formation of $OH{:}e^-$ pairs as a precursor of the reported fast relaxation to a hot anion ground state.[22] Most important, almost half of those pairs recombine on the subpicosecond time scale. Both the quantum yield and the time constant of this process show an isotope effect of 1.4.

2. EXPERIMENTAL DETAILS

The laser system used in the present study was described recently.[38] A homemade Ti:sapphire laser provides pulses at 810 nm with energy of 400 μJ, pulse duration of 90 fs, and repetition rate of 1 kHz. The electron photodetachment is initiated by linear absorption at 202 nm. The changes of optical density, ΔOD, induced in the samples are monitored by probe pulses tunable in a wide spectral range from 450 nm to 2.45 μm. The width of the intensity cross-correlation function was approximately 150 fs in the VIS and NIR, and somewhat larger for probe wavelengths beyond 2 μm. The secondary excitation is achieved by 1-photon absorption at 810 nm induced by a fraction of the laser pulse at low intensity level. The PREP-signal Δ(ΔOD) discussed below represents the difference of probe absorption changes measured after two-pulse excitation (pump and repump) and for single-pulse excitation (repump pulse blocked) by the help of two chopper wheels in the excitation beams.

The OH^- sample consists of KOH (80 mM) in tridistilled water. The OD^-_{aq} solution was prepared from KOD (80 mM) and D_2O with purities of 98 atom % and 99.9 atom % deuterium, respectively. In order to maintain a constant sample temperature, the solution passes a heat exchanger. The solvent temperature was controlled via an electronic contact thermometer right before passing the free-flow sample jet (100 μm thickness). The experiments are performed at various temperatures in the range from 280 to 335 K. To prevent proton exchange (primarily due to air humidity) the sample jet was flushed with nitrogen throughout the measurement. A fresh sample was prepared for every experimental session.

3. RESULTS

Time-resolved data measured after UV excitation of OH^- in water are shown in Figure 1 (see also Figures S1 and S3 in the Supporting Information). The solvent temperature was 297 K. The temporal evolution of the absorption changes is depicted as a contour plot in Figure 1a, with the color code given next to Figure 1c. The ordinate scale in Figure 1a shows the probe photon energy, while the abscissa indicates the pump−probe delay time t_{13}. Note that the delay time is given on a linear scale up to 2 ps and on a logarithmic scale for larger values. The transient spectra measured for a few fixed delay times are presented in Figure 1b. The induced absorption in Figure 1 for $t_{13} > 200$ fs is assigned to excess electrons, since the OH radicals do not show up in the displayed spectral range.[22]

At short delay times a rapid absorption increase is measured with a maximum in the mid-infrared. The signal transients presented in Figure S1 of Supporting Information show that the instantaneous rise in the near- and mid-infrared is followed by rapid decay with a time constant below 200 fs. In contrast, the transient signals measured in the visible display a significantly slower increase, peaking at about 0.5 ps. These observations give an upper limit of 200 fs for the lifetime of the initially excited CTTS state. We mentioned that the probe absorption measured upon the UV excitation contains a minor signal component due to the so-called pump−probe coherent artifact.[39,40] The effect is expected to be larger for probing close to the excitation wavelength.[40] By comparison with data for a neat water sample we find that the coherent artifact is small and is taken into account in the data analysis below.

By increasing the delay time the emerging absorption band, that is assigned to detached electrons, narrows significantly and shifts to higher probe frequencies (see also Figure S3 of Supporting Information). An important property of the solvated electron is the high sensitivity of its absorption spectrum to the local environment.[25,41] Thus, the continuous blue shift of the e^-_{hyd}-absorption spectrum is often assigned to a fast local cooling of the electron solvation shell.[25,42,43] The heat dissipation of the first solvent shell is believed to be involved in the fast spectral blue-shift observed in the first few picoseconds (see Figure 1b and also Figure S3 of Supporting Information). The time evolution of the spectral shift terminates ~3 ps after the UV excitation pulse, arriving at the well-known absorption spectrum of e^-_{hyd} centered at 1.72 eV (720 nm).[41]

The transient dynamics measured for delay times beyond 3 ps only involve an amplitude decay with a constant band shape. According to similar studies on various CTTS systems,[24−31] the latter process is assigned to recombination/dissociation of a solvent-separated pair $(OH{:}e^-)_{aq}$ and later on also to diffusive

dx.doi.org/10.1021/ja103866s |J. Am. Chem. Soc. 2011, 133, 790–795

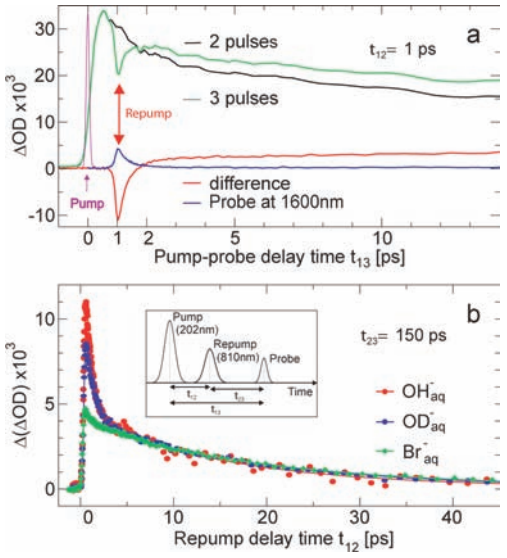

Figure 2. (a) Probe absorption changes at 700 nm (black line) induced in OH^-_{aq} solely by the UV pump pulse (indicated schematically by the violet dotted curve); same with an additional weak repump pulse at 810 nm with fixed delay of 1 ps after the UV pump (green). The difference Δ(ΔOD) of both signals (green − black) represents the PREP signal shown in red. The repump-induced absorption changes for probing at 1600 nm are presented in blue for comparison. (b) PREP data taken at 700 nm and various repump delay t_{12}. Probe delay t_{23} is fixed at 150 ps. Transients measured in OH^-_{aq} (blue), OD^-_{aq} (red), and Br^-_{aq} (green) at 297 K. The pulse sequence, wavelengths, and definition of delay times for the PREP measurements are illustrated by the inset. Experimental points, calculated solid lines.

recombination of fully released electrons.[20] The anticipated pair complex is stabilized by a weak attractive potential ($3-4k_BT$), and its dissociation is controlled by thermal fluctuations.[20,24,27−29] The pair intermediate displays a similar spectral signature as e^-_{hyd}. It is believed that the electron and the radical are separated by at least one water molecule.[32] Thus, the electron is equipped with a complete nearest neighbor shell of solvent molecules that govern its spectral properties.

Pump−probe measurements in OD^-_{aq} were carried out under the same experimental conditions (see also Figures S2 and S4 of Supporting Information). The observed dynamics are similar to those in OH^-_{aq}, except for an increased quantum yield of long-lived solvated electrons. The signal transients measured close to the absorption maximum of e^-_{hyd} are presented in c and d of Figure1. The induced absorptions reach almost the same maximum in both samples (see Figure 1d). The peak is followed by a rapid signal decrease. The initial decay measured in OH^-_{aq} (~0.7 ps) is faster and more pronounced than that observed in OD^-_{aq} (~1.0 ps). The mechanism governing the fast loss of e^-_{hyd}-absorption is not obvious on the basis of the pump−probe data. The subsequent slower decay measured in both samples is similar. The latter feature is shown in Figure 1c, where the OD signal is scaled by a factor of 0.8. This signal decay displays a time constant of about 15−20 ps and is assigned to recombination of a solvent-separated pair $(OH:e^-)_{aq}$.[20] The subnanosecond dynamics are associated with diffusion-controlled recombination between free electrons and OH radicals.

To elucidate the relaxation pathway in more detail, we utilized pump−repump−probe (PREP) spectroscopy. The technique was introduced by Schwartz and co-workers for optical manipulation of electron transfer processes.[44−46] In an analogous manner we apply a second excitation pulse at 810 nm to study the OH and electron quenching. The repump wavelength is suitable for selectively exciting e^-_{hyd},[41] since neither the solvent nor OH^- or OH absorb notably in this spectral range.[22] The pulse sequence and the definition of repump delay, t_{12}, and probe delay, t_{23}, used for the PREP measurements are illustrated in the inset of Figure 2b. The probe absorption changes measured in OH^-_{aq} with the repump pulse fixed at t_{12}=1 ps after the UV pump pulse are presented by the green line in Figure 2a. The data are collected at 700 nm and for various pump−probe delay times t_{13}. The black line is measured by standard pump−probe technique (repump pulse blocked). The PREP-signal Δ(ΔOD) represents the difference between both probe absorptions (red curve in Figure 2a).

The PREP data measured at t_{13} = 1 ps, i.e. simultaneously with the repump pulse, indicate a relative signal bleaching at 700 nm due to a population decrease of the ground state of e^-_{hyd}.[47] The first excited state of the electrons is characterized by an induced absorption in mid-infrared[48] and was monitored exemplarily at 1600 nm (blue line in Figure 2a). Similar dynamics were also observed for shorter pump−repump delay times t_{12} < 1 ps. Recalling the short lifetime of the CTTS state (below 200 fs) the observations give strong evidence that the repump pulse at 810 nm addresses mainly the excess electrons in the sample, while a CTTS excited-state absorption appears to be of minor importance.

The excited electron relaxes within 200 fs to a `hot' ground state, and the excess energy is transferred to the solvent environment.[48] The resulting local heating is believed to represent an important factor increasing the mobility of the relaxing electron.[38,49] The higher mobility allows the electron to escape from the adjacent quencher, i.e. the OH radical. Thus, the repump process converts solvent-separated pairs $(OH:e^-)_{aq}$ into freely diffusing electrons and donors.[38,44] Correspondingly, the absorption signal at 700 nm measured for longer t_{13} becomes larger with secondary excitation than without a repump pulse (note green curve in Figure 2a).

Particularly important are the data shown in Figure 2b for large probe delay, t_{23} = 150 ps, and variable repump delay t_{12}. The absorption rise observed here is a measure for the repump-induced increase in the number of e^-_{hyd} that escape the recombination process.[38] The PREP signal transients taken in OH^-_{aq} (blue) and OD^-_{aq} (red) indicate two distinct relaxation time constants. The data strongly suggest that two mechanisms are involved in the dynamics. (As discussed above, the strong repump effect channel cannot be explained by excited-state absorption of the CTTS state at 810 nm.) The finding represents strong evidence that both channels are due to geminate recombination of partially and/or fully solvated electron and OH radicals. The fast recombination in Figure 2b displays a clear isotope effect and is not observed in aqueous bromide Br^-_{aq} (see green line in Figure 2b and ref 38).

The slower decays measured in all three samples are similar and are attributed to solvent-separated electron-donor pairs.[20,22,38] The pair lifetime decreases for higher temperatures (see Figure S5 in Supporting Information). The observation agrees with other results on OH^-_{aq}[20,22] and is consistent with an activation energy governing the recombination of OH−electron pairs. No temperature dependence of the fast channel is found within our experimental accuracy.

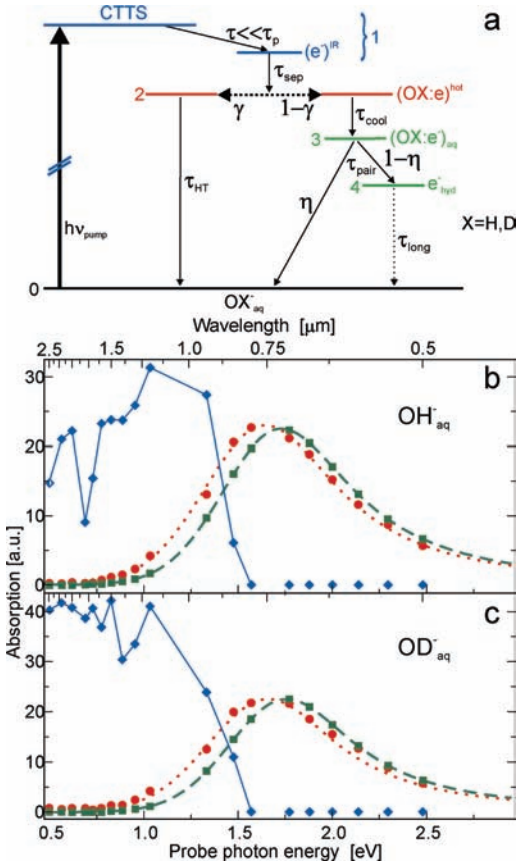

Figure 3. (a) Simplified relaxation model for the photogeneration of the OH and OD radicals that accounts for the measured dynamics. (b) Absorption signatures of the intermediates involved in the photodetachment of OH^-_{aq} deduced from the experimental data by the help of the model (data points). First intermediate (1) (blue diamonds), the hot solvent-separated radical-electron pair $(OH:e^-)^{hot}$ (precursor (2), red points), and to the equilibrated pair $(OH:e^-)_{aq}$ (intermediate (3)) together with that of the hydrated electron e^-_{hyd} (4) (green squares). (c) Same as (b) but for the OD^- in heavy water. The lines are guides to the eye (see text). The determined spectral signatures support the assignment of species (1) to (4).

4. DISCUSSION

Our experimental data are analyzed with the help of a five-level model schematically shown in Figure 3a. The model extends earlier approaches on OH^-_{aq}[20−22] and Br^-_{aq}[38] to account for the novel fast recombination channel reported here. We have computed the numerical solutions of rate equations describing the relaxation model of Figure 3a, taking also the finite durations of the pump, repump, and probing pulses properly into account. The time constants, quantum yields, and absorption cross sections of intermediates are treated as adjustable parameters. The absorption cross section of the final species, i.e. the hydrated electron, is taken from the data of Jou and Freeman[41] for H_2O and D_2O (see green dashed lines in b and c of Figure 3, respectively). In this way the relative amount of absorbing species is determined. A global fit to pump−probe and PREP data is carried out. The extracted spectral signatures of the involved intermediates (fitted absorption cross sections) are depicted as data points in b and c of Figure 3 for OH^-_{aq} and OD^-_{aq}, respectively. They represent important information and support the assignment of the intermediates. The fit also yields the time constants and quantum yields of the model.

The UV pump pulse promotes hydrated anions OX^-_{aq} (X = H, D) from the ground state (level 0) to the lowest CTTS state. The relaxation of the latter state may occur within our experimental time resolution to a possible first species. Both states are combined in the model to a precursor (1) that is characterized by a decay time $\tau_{sep} = 160 \pm 50$ fs. Intermediate (1) displays a broad absorption extending from 800 nm beyond 2.5 μm (blue diamonds in b and c of Figure 3) and is assigned to an initial solvation of the released electron.[10]

Subsequently, a charge-separated precursor (2) is formed that is believed to represent nonequilibrated solvent-separated pairs $(OX:e^-)^{hot}$.[25,38] As a strong simplification, the adiabatic thermalization process is only accounted for by a discrete state with a (time-) averaged absorption spectrum (red points in b and c of Figure 3) and time constant τ_{cool}. Intermediate (2) shows almost the same spectral signature and oscillator strength as e^-_{hyd} for a higher solvent temperature of 335 ± 10 K (see calculated red dotted lines in a and b of Figure 3).[41] The finding supports the assignment of the precursor.

For the relaxation of species (2) a branching with two decay channels is introduced. A fraction γ of the hot pairs returns to the (hot) ground state (0) with a decay time τ_{HT}. The process represents the fast decay, i.e. recombination channel, observed in the PREP data. Our model is consistent with the recent study on photodetachment of OH^-_{aq}, where a fast relaxation to `hot' OH^-_{aq} was reported.[22] The quantum yield ($\gamma = 0.49 \pm 0.05$ for $OH:e^-$ and 0.35 ± 0.05 for $OD:e^-$) and the time constant ($\tau_{HT} = 0.7 \pm 0.2$ and 1.0 ± 0.2 ps for OH and OD, respectively) of the novel channel display an isotope effect of approximately 1.4. These numbers are in amazingly good agreement with the experimentally observed difference of the PREP signal amplitudes measured for OH^- and OD^- (see Figure 2a), when the different absorption cross sections for the two cases are taken into account. The finding supports the physical picture developed here.

To account for the thermalization process, the model assumes that the main part $(1-\gamma)$ of the hot $OH:e^-$ pairs (2) equilibrates to intermediate (3), assigned to $(OX:e^-)_{aq}$. The time constant of the relaxation is determined to $\tau_{cool} = 1.4 \pm 0.2$ ps for OH and 1.5 ± 0.2 ps for OD, respectively. The pair species display the well-known absorption band of e^-_{hyd} (green rectangles) in the VIS and NIR.[20,41] The major part of the equilibrated pairs ($\eta = 0.69 \pm 0.05$ for OH and 0.71 ± 0.05 for OD) recombines rather slowly with an effective lifetime $\tau_{pair} = 14.5 \pm 2$ ps and 18 ± 2 ps for OH and OD at 298 K, respectively. The latter dynamics are strongly temperature dependent, and for the OH case τ_{pair} decreases from 19 ± 2 ps to 9 ± 1 ps going from 280 to 335 K. The dissociation of pairs (3) leads to fully detached electrons e^-_{hyd} (level 4). The latter disappear again in part due to free diffusive recombination with an effective time constant $\tau_{long} > 1.5$ ns.

The observed high recombination quantum yield of the nonequilibrated $OH:e^-$ pair agrees with the high reactivity of the not fully hydrated (prehydrated) electrons, reported recently.[5,7] The reactivity of the prehydrated electron could also play an important role in the significant loss channel competing with the electron detachment process in aqueous fluoride.[37] Moreover, the measured recombination time between the electron and the fluorine atom[37] of 430±80 fs is similar to the reported lifetime of the prehydrated electron of 200−500 fs.[5,10,39,50]

As mentioned above, the fast geminate recombination was not observed in similar measurements in Br^- and I^- (data not

dx.doi.org/10.1021/ja103866s | J. Am. Chem. Soc. 2011, 133, 790–795

shown). Therefore, it could be surmised that this process is uniquely connected to the properties of the hydroxyl anion. A possible mechanism is an ultrafast transfer of an H-atom from a neighboring water molecule, thus providing an enhanced interaction between the excess electron and the OH radical. Car−Parrinello simulations[51] predict that H-transfer occurs if the OH radical possess three H-bonds in an almost ideal tetrahedral configuration, i.e. similar to the solvation shell of the anion OH^-.[11−13] The low probability of such solvent configurations, in general, reduces the H-transfer rate.[52] However, immediately after the photodetachment the OH radical is solvated in the original anion solvent cavity. The rearrangement and equilibration of the solvent environment, however, terminates the H-transfer. In fact, the predicted[51] average H-bond's lifetime of about 0.7 ps resembles the time constant of the fast recombination channel. The quantum yield and rate of the H-transfer process are connected with the stretching vibration of the water molecule.[52] The latter point is consistent with the measured isotopic effect. At this time, however, the mechanism of the observed fast geminate recombination cannot be extracted from our data. This is a challenging problem for theoretical investigations that will hopefully be conducted in the near future.

5. CONCLUSIONS

We report on the photodetachment of OH^-_{aq} and OD^-_{aq} at 202 nm. The recombination dynamics are studied with two- and three-pulse spectroscopy. An early intermediate is observed that builds up within 160 fs and is assigned to nonequilibrated OH− electron pairs. The subsequent dynamics are governed by equilibration, recombination, and dissociation of the pairs. The latter process yields the final hydrated electrons and hydroxyl radicals. An additional pulse at 810 nm is used for secondary excitation of the intermediate species. Using this technique we observe a novel geminate recombination channel of OH with adjacent hydrated electrons. The process leads to an ultrafast quenching (700 fs) of almost half the initial number of radicals. The fast mechanism displays an isotope effect of 1.4 for both quantum yield and lifetime. Of the $(OD{:}e^-)$ pairs, 35% recombine with a time constant of 1.0 ps. Our findings demonstrate the high reactivity of the prehydrated electron. The phenomenon is not observed in similar experiments on aqueous bromide and seems to be anion-related. An ultrafast interaction of OH with neighboring water molecules involving a transfer of H atoms is discussed as a possible bottleneck of the novel geminate recombination channel.

■ ASSOCIATED CONTENT

Supporting Information. Figures S1 and S2 showing pump−probe signal transients measured in OH^-_{aq} and OD^-_{aq}, respectively, for different probe wavelengths; Figures S3 and S4 illustrating transient spectra taken at selected pump−probe delay times; Figure S5 presenting pump-repump−probe data measured at various solvent temperatures. This material is available free of charge via the Internet at http://pubs.acs.org/.

■ AUTHOR INFORMATION

Corresponding Author
hristo.iglev@ph.tum.de

■ ACKNOWLEDGMENT

This work was supported by Deutsche Forschungsgemeinschaft, Project IG81/2-1.

■ REFERENCES

(1) Lehnert, S. *Biomolecular Action of Ionizing Radiation*; Taylor & Francis Group: New York, 2008.
(2) Suthanthiran, M.; Solomon, S. D.; Williams, P. S.; Rubin, A. L.; Novgorodsky, A.; Stenzel, K. H. *Nature* **1984,** *307*, 276.
(3) Atinault, E.; De Waele, V.; Schmidhammer, U.; Fattahi, M.; Mostafavi, M. *Chem. Phys. Lett.* **2008,** *460*, 461.
(4) Boudaiffa, B.; Cloutier, P.; Hunting, D.; Huels, M. A.; Sanche, L. *Science* **2000,** *287*, 1658.
(5) Wang, C.-R.; Nguyen, J; Lu, Q.-B. *J. Am. Chem. Soc.* **2009,** *131*, 11320.
(6) Sanche, L. *Nature* **2009,** *461*, 358.
(7) Wang, C.-R.; Lu, Q.-B. *Angew. Chem., Int. Ed.* **2007,** *46*, 6316.
(8) Hahn, P. H. *Phys. Rev. Lett.* **2005,** *94*, 037404.
(9) Elles, C. G.; Jailaubekov, A. E.; Crowell, R. A.; Bradforth, S. E. *J. Chem. Phys.* **2006,** *125*, 044515.
(10) Laenen, R.; Roth, T.; Laubereau, A. *Phys. Rev. Lett.* **2000,** *85*, 50.
(11) Tuckerman, M. E.; Marx, D.; Parrinello, M. *Nature* **2002,** *417*, 925.
(12) Sun, X.; Yoo, S.; Xantheas, S. S.; Dang, L. X. *Chem. Phys. Lett.* **2009,** *481*, 9.
(13) Aziz, E. F.; Ottosson, N.; Faubel, M.; Hertel, I. V.; Winter, B. *Nature* **2008,** *455*, 89.
(14) Roberts, S. T.; Petersen, P. B.; Ramasesha, K.; Tokmakoff, A.; Ufimstev, I. S.; Martinez, T. J. *Proc. Natl. Acad. Sci. U.S.A.* **2009,** *106*, 15154.
(15) Robertson, W. H.; Diken, E. G.; Price, E. A.; Shin, J. W.; Johnson, M. A. *Science* **2003,** *299*, 1367.
(16) Thorgersen, J.; Jensen, S. K.; Petersen, C.; Keiding, S. R. *Chem. Phys. Lett.* **2008,** *466*, 1.
(17) Smith, J. R.; Kim, J. B.; Lineberger, W. C. *Phys. Rev. A* **1997,** *55*, 2036.
(18) Winter, B.; Faubel, M.; Hertel, I. V.; Pettenkofer, C.; Bradforth, S. E.; Jagoda-Cwiklik, B.; Cwiklik, L.; Jungwirth, P. *J. Am. Chem. Soc.* **2006,** *120*, 3864.
(19) Fox, M; McIntyre, R.; Hayon, E. *Faraday Discuss* **1977,** *64*, 167.
(20) Crowell, R. A.; Lian, R.; Shkrob, I. A.; Bartels, D. M.; Chen, X.; Bradforth, S. E. *J. Chem. Phys.* **2004,** *120*, 11712.
(21) Lian, R.; Crowell, R. A.; Shkrob, I. A.; Bartels, D. M.; Oulianov, D. A.; Goszola, D. *Chem. Phys. Lett.* **2004,** *389*, 379.
(22) Petersen, R.; Thogersen, J.; Jansen, S. K.; Keiding, S. R. *J. Phys. Chem. A* **2007,** *111*, 11410.
(23) Bradforth, S. E.; Jungwirth, P. *J. Phys. Chem. A* **2002,** *106*, 1286.
(24) Chen, X.; Bradforth, S. E. *Annu. Rev. Phys. Chem.* **2008,** *59*, 203.
(25) Iglev, H.; Trifonov, A.; Thaller, A.; Buchvarov, I.; Fiebig, T.; Laubereau, A. *Chem. Phys. Lett.* **2005,** *403*, 198.
(26) Shkrob, I. A. *Chem. Phys. Lett.* **2004,** *395*, 264.
(27) Sauer, J., M. C.; Crowell, R. A.; Shkrob, I. A. *J. Phys. Chem. A* **2004,** *108*, 5490.
(28) Sauer, J., M. C.; Shkrob, I. A.; Lian, R.; Crowell, R. A.; Bartels, D. M.; Chen, X.; Suffern, D.; Bradforth, S. E. *J. Phys. Chem. A* **2004,** *108*, 10414.
(29) Lian, R.; Oulianov, D. A.; Crowell, R. A.; Shkrob, I. A.; Chen, X.; Bradforth, S. E. *J. Phys. Chem. A* **2006,** *110*, 9071.
(30) Kloepfer, J. A.; Vilchiz, V. H.; Lenchenkov, V. A.; Bradforth, S. E. *Chem. Phys. Lett.* **1998,** *298*, 120.
(31) Kloepfer, J. A.; Vilchiz, V. H.; Lenchenkov, V. A.; Chen, X. Y.; Bradforth, S. E. *J. Chem. Phys.* **2002,** *117*, 766.
(32) Staib, A.; Borgis, D. *J. Chem. Phys.* **1996,** *104*, 9027.
(33) Sheu, W. S.; Rossky, P. J. *J. Phys. Chem.* **1996,** *100*, 1295.
(34) Vassilev, P.; Louwerse, M. J.; Baerends, E. J. *J. Phys. Chem. B* **2005,** *109*, 23605.

(35) Adriaanse, C.; Sulpizi, M.; VandeVondele, J.; Sprik, M. *J. Am. Chem. Soc.* **2009,** *131,* 6046.
(36) Khalack, J. M.; Lyubartsev, A. P. *J. Phys. Chem. A* **2005,** *109,* 378.
(37) Iglev, H.; Laenen, R.; Laubereau, A. *Chem. Phys. Lett.* **2004,** *389,* 427.
(38) Fischer, M. K.; Laubereau, A.; Iglev, H. *Phys. Chem. Chem. Phys.* **2009,** *11,* 10939.
(39) Wang, C.-R.; Luo, T.; Lu, Q.-B. *Phys. Chem. Chem. Phys.* **2008,** *10,* 4463.
(40) Kovalenko, S. A.; Ersting, N. B.; Ruthmann, J. *Chem. Phys. Lett.* **1996,** *258,* 445.
(41) Jou, F.-Y.; Freeman, G. R. *J. Phys. Chem.* **1979,** *83,* 2383.
(42) Madsen, D.; Thomsen, C. L.; Thogersen, J.; Keiding, S. R. *J. Chem. Phys.* **2000,** *113,* 1126.
(43) Lindner, J.; Unterreiner, A.-N.; Vöhringer, P. *ChemPhysChem* **2006,** *7,* 363.
(44) Martini, I. B.; Barthel, E. R.; Schwartz, B. J. *J. Am. Chem. Soc.* **2002,** *124,* 7622.
(45) Martini, I. B.; Barthel, E. R.; Schwartz, B. J. *Science* **2001,** *293,* 462.
(46) Bragg, A. E.; Cavanagh, M. C.; Schwartz, B. J. *Science* **2008,** *321,* 1817.
(47) Silva, C.; Walhout, P. K.; Yokoyama, K.; Barbara, P. F. *Phys. Rev. Lett.* **1998,** *80,* 1086.
(48) Thaller, A.; Laenen, R.; Laubereau, A. *Chem. Phys. Lett.* **2004,** *398,* 459.
(49) Schmidt, K. H.; Han, P.; Bartels, D. M. *J. Phys. Chem.* **1992,** *96,* 199.
(50) Assel, M.; Laenen, R.; Laubereau, A. *J. Chem. Phys.* **1999,** *111,* 6869.
(51) Khalack, J. M.; Lyubartsev, A. P. *J. Phys. Chem. A* **2005,** *109,* 378.
(52) Arnaut, L. G.; Formosinho, S. J.; Barroso, M. *J. Mol. Struct.* **2006,** *786,* 207.